Long-term impact of air pollutants on thermochemical heat storage materials

Simona Bennici, Téo Polimann, Michel Ondarts, Evelyne Gonze, Cyril Vaulot, Nolwenn Le Pierrès

Long-term impact of air pollutants on thermochemical heat storage materials

Bennici Simona[2,3,*], Polimann Téo[1], Ondarts Michel[1], Gonze Evelyne[1], Vaulot Cyril [2,3], Le Pierrès Nolwenn[1]

[1] LOCIE, CNRS UMR 5271, Université Savoie Mont-Blanc, 73376 Le Bourget du Lac, France
[2] Université de Haute-alsace, CNRS, IS2M UMR 7361, F-68100 Mulhouse, France
[3] Université de Strasbourg, France
* Corresponding author details: simona.bennici@uha.fr; Tel.: +33-389-336-729

Abstract

Heating of buildings is a highly energy-demanding task. Therefore, improving energy management is crucial for more environmentally friendly development of future constructions, and the use of thermochemical heat storage technologies in solid materials is one of the most promising solutions. Nevertheless, certain drawbacks such as the impact of air pollutants on the long term durability of thermochemical heat storage materials (ageing up to 30 years) need to be studied to implement installations. In certain thermochemical heat storage systems, air passes through porous materials to carry water and heat, and the air's pollutants can interact with the solid material, thus decreasing its storage capacity.

In the present work, adsorption tests were performed (under dynamic conditions) on zeolite-base materials, using different model molecules (i.e. toluene, styrene and hexaldehyde) representative of air pollutants. Strong competition between the adsorption of pollutants and water on the storage material was demonstrated. Water molecules were able to displace the molecules of pollutants, previously adsorbed on the material surface, thus delaying the saturation of the material and extending its life. Nevertheless, a lowering of the water adsorption and heat storage capacity was measured for a high number of cycles. The cycled materials have been thoroughly characterised in their physicochemical properties to identify the modifications of the materials (i.e., de-alumination) and correlate them with the heat storage capacity. The impact of pollutants was demonstrated to be stronger on the pure

zeolite, while the salt present on the $MgSO_4$/13X composite seems to protect the material surface from the pollutant effect.

Highlights

- The zeolite-base materials are highly stable in hydration/dehydration cycles
- The heat storage capacity decreases in presence of pollutants
- Pollutant molecules are displaced by water molecules during hydration
- The microstructure of the material is modified during cycles

Key words: thermochemical storage; pollution; energy recovery; solar energy; zeolites; material characterisation.

Word Count: 4184

Declaration of interest: none.

Abbreviations: $\mathcal{H}$, relative humidity; FID, flame ionisation detector; FTIR, Fourier-transform infrared spectroscopy; WDXRF, wavelength dispersive x-ray fluorescence; XPS, x-ray photoelectron spectroscopy; BE, binding energy; BET, Brunauer Emmett and Teller; SSA, specific surface area; MAS, magic angle spinning; NMR, nuclear magnetic resonance; TG-DSC (thermogravimetry-differential scanning calorimetry); IR, infrared; S_{BET}, BET specific surface area; S_{micro} micropore specific surface area; V_{tot}, total pore volume; $V_{micro,}$ micropore volume

1. Introduction

To decrease the dependence on fossil energy sources (expensive, limited and polluting), the solution is to orient development towards the use of renewable energies, which can be implemented in more environmentally friendly solutions [1,2]. Solar energy is the most abundant renewable energy source. Unfortunately, solar energy is intermittent, and, consequently, the need to bridge the gap between energy supply and energy demand remains a challenge. For this reason, identifying, developing, and optimising the energy storage technologies is the entryway to a renewable energy-based economy [2-3]. Solar power peak availability occurs during the day and summer, periods during which the heating demand in buildings (for sanitary hot water and building heating) is at its lowest. Storage systems are therefore necessary to store the excess heat produced during sunny periods, to be used during the periods of highest demand [4]. Thermal energy storage can be applied by means of different specific technologies: water, phase-change materials, and thermochemical reactions [2,5]. These technologies can be based on different physicochemical phenomena. The most widely used systems are based on the exploitation of sensible heat, linked to the heat exchanged due to changes in the system's temperature [6]. Currently, water is widely used for sensible heat storage; however, for building heating applications and long-term storage, excessively large volumes are required, and its application is unrealistic for a small family home, for example [7]. The second solution is based on latent heat storage; in this case the heat stored/released by the material stems from a phase change. The third way, which is considered in the present study, is thermochemical heat storage, based on reversible chemical reactions (for example hydration/dehydration of a material) [2, 3]. Systems based on this principle have the advantage of presenting negligible heat loss during storage and having a higher heat density than the other storage systems mentioned above. The main advantage of using this type of system is the possibility of storing heat during the period of energy availability (e.g. solar radiation) to perform the charging step (i.e. dehydration of the solid

material) and release it (i.e. hydration of the solid) for utilisation in the desired application (house heating), as shown in Fig. 1.

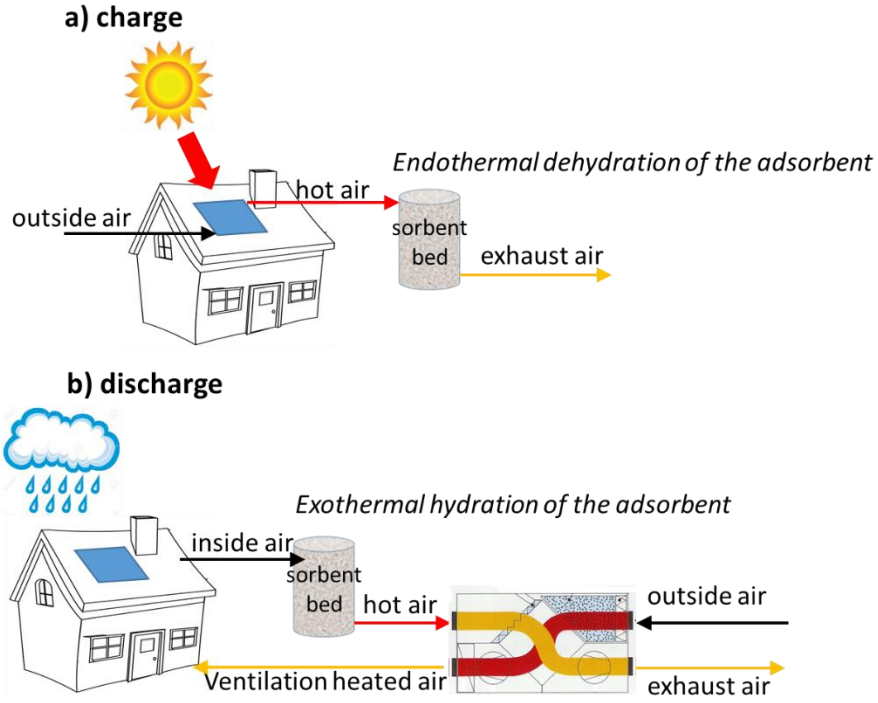

Fig. 1. *Principle of the adsorption heat storage system functioning (a) charging step: endothermal dehydration of the adsorbent using air heated by a solar collector; (b) discharging step: heating of the ventilation air by exothermal hydration of the adsorbent*

The solid storage material is at the heart of such thermochemical heat storage systems, and it must possess certain specific properties [8], such as high energy density, high affinity for the sorbate, water (to ensure the exothermic chemical reaction), high thermal conductivity (to facilitate heat transfer and recovery), a high heat transfer coefficient with the heat transfer fluid, and a desorption (dehydration) temperature as low as possible. Moreover, the storage materials must be environmentally friendly, non-toxic, non-corrosive, inexpensive, and present good thermal and chemical stability under operating conditions (temperature, pressure, etc.). Various authors have explained that the main disadvantage of such materials is the limitation in heat and mass transfer [8]. The main limitation in solid adsorbents is the low

thermal conductivity of sorbents and the possibility of crust formation (in case salts are used), which limits water diffusion. Despite these drawbacks, several sorption couples have been identified and studied for the implementation of the process. Three main families of porous materials (mesoporous silicates, zeolites and metal aluminophosphates) have been widely reported in the literature [2,3]. Among them, zeolites are the best choice for large-scale and long-term applications, due to their high heat storage capacity and durability [9,10].

In certain types of thermochemical heat storage installations (such as that considered in the present study), air passes through the porous material to carry water (the sorbate) and heat (Fig. 1). It is therefore necessary to study the impact of air pollutants (indoor and outdoor air) [11-13] on the ageing of these materials. In the long term (functioning over 30 years), these pollutants can interact with the solid and eventually decrease the material's storage capacity. Outdoor and indoor air pollutants are mainly composed of solid particles, inorganic (ozone, nitrogen oxides) and organic pollutants (volatile organic compounds and carbonyl compounds). Their concentrations vary from a few $\mu g.Nm^{-3}$ up to a few hundred $\mu g.Nm^{-3}$ [12,13]. The present study focuses only on chemical pollutants. Moreover, zeolites are known to be good adsorbents for atmospheric pollutants [14,15], and their affinity for these molecules might be a drawback for their application in real thermochemical heat storage systems.

In this study, the impact of air pollutants on the durability of thermochemical heat storage materials has been examined, because, to our knowledge, no research concerning the impact of pollution on these systems and their heat storage performance has been reported to date in the literature. Critical pollutants were chosen and ageing tests were performed to model the storage material implementation in a long-term application and in successive hydration/dehydration cycles. Adsorption tests (performed under static and dynamic conditions) were carried out on zeolite-base materials (13X pure zeolite and a $MgSO_4$/13X

composite), using different molecules representative of the pollutants (toluene, styrene and hexaldehyde), chosen as model molecules.

Then the cycled materials were deeply characterised to shed light on the changes in their properties and correlate them with the loss in heat storage capacity.

2. Material and methods

2.1. Zeolite, composite and pollutants

Commercial 13X zeolite (supplied by Chemiewerk Bad Köstritz GmbH, brand Köstrolith 13XBF K distribution), shaped in spheres 1.2 to 2.0 mm in diameter, was chosen as the sorbent solid material, the sample was labelled 13X. This type of zeolite has been widely studied in thermochemical heat storage processes [16,17].

A second sample, a composite, was prepared by depositing 15 wt% $MgSO_4$ (99.5% purity, purchased from Sigma-Aldrich) on the 13X zeolite, used as the support, using the impregnation method under vacuum, with the same procedure and the same vacuum apparatus as reported in Ref. [10], and labelled $MgSO_4$/13X. A large comparison of the possible thermochemical heat storage materials (mainly salts hydrate) was carried out at ECN (Energy research Center of the Netherlands and reported in 2004 [18] whereby $MgSO_4$ was identified as a potential material for long-term heat storage thanks to its theoretical high storage density of 780 $kWh.m^{-3}$. During hydration/dehydration, $MgSO_4$ can be present in different hydrated forms [7,19] and under practical conditions it cannot release the total theoretical amount of heat stored. Nevertheless, even if not completely hydrated/dehydrated, magnesium sulphate represents a good choice for heat storage, when its dispersion on a support allows to overcome the diffusion water issues present in the bulk salt [18-20]. Moreover, $MgSO_4$ is also non-toxic, relatively cheap and non-corrosive, which are very important properties for a material that might be used at large scale in households' applications.

The possibility to efficiently deposit $MgSO_4$ on zeolites was already demonstrate in previous researches [19]. In the same research, loading 15wt% of $MgSO_4$ on the zeolites was shown to be the best compromise to obtain the highest increasing of the heat storage capacity and preserve the zeolite porosity.

Three representative air pollutants were selected on the basis of Ref. [11]: toluene (99.9% purity, Fisher Scientific, Leicestershire, UK), styrene 99.5% purity, Acrôs Organics) and hexaldehyde (96% purity, Acrôs Organics). The three pollutants have been selected among the others present in indoor air due to their different physico-chemical properties and chemical reactivity. Toluene is a synthetic intermediate for the manufacture of many products: benzene, xylenes, phenol, etc. It is also largely present in solvents for paints, varnishes, printing inks, glues, waxes, etc. Toluene is therefore present in large quantities in indoor air. Moreover, it is almost not soluble in water. Lee et al. [21] enlightened the possible adsorption of toluene on zeolite. In this study, industrial effluents loaded with toluene and acetone were treated with a Y-type zeolite. Toluene desorption was obtained in the 150- 180°C interval, indicating the formation of chemical bonds between toluene and zeolite. Knowing that in the solar storage process the expected temperature in the charge phase is 165°C, the study of toluene will allow to verify if the charging temperature is higher enough to avoid the accumulation of this compounds on the storage material. Styrene is present in small quantities in most indoor environments due to its desorption from plastic materials, glues, paints, solvents, etc. It is not miscible with water as toluene, but present the particularity of being higly reactive: it polymerises and oxidizes very easily. The polymerization reaction is accelerated by the action of light and heat. Barson et al. [22] showed that starting from 30°C styrene polymerizes on zeolite 13X. For this reason, styrene has been chosen as model pollutant to investigate the possible blocking of the zeolite pores due to the formation of polymerisation products and sub-products. Finally, hexanal is an organic compound of the aldehydes family. It is present in

most perfumes and aromas, because it is used in the extraction process. Hexanal was selected for this study because is a persistent pollutant present in relatively high quantities in indoor air, and because, being very miscible with water, it might reach in depth the micropores of the storage material during the adsorption phase.

2.2. Pollutant adsorption – breakthrough curves and cycling tests

The acquisition of the breakthrough curves of the three pollutants on the zeolite and composite, as well as hydration/dehydration cycles, were performed in continuous flow mode. These breakthrough curves are widely applied methods to evaluate the performance of adsorption storage systems, as described in [20] or [23]. In our case, dry (relative humidity $\mathcal{H}$ < 1%) and humidified air ($\mathcal{H} \approx$ 60%) flows) were used to represent the charging and discharging steps of the real system. The experimental set-up used is shown in Fig. 2.

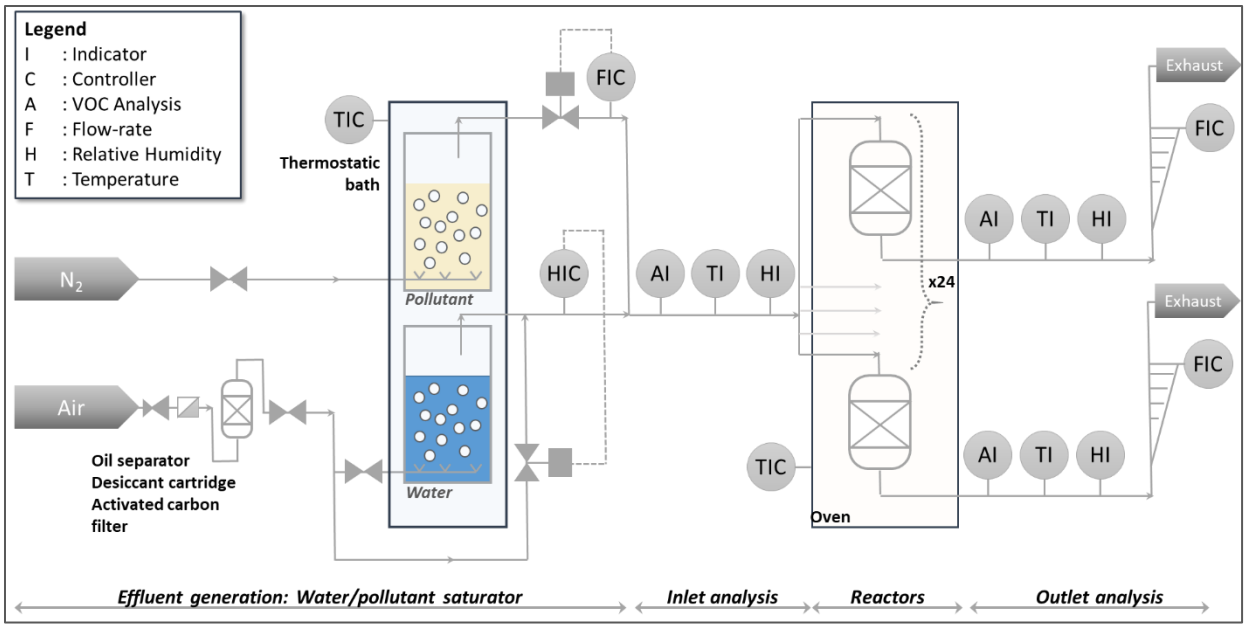

Fig. 2. *Scheme of the experimental set-up.*

The carrier gas (atmospheric compressed air) was purified and dried using an oil separator, a desiccant cartridge, an activated carbon filter and a particulate filter. In the experiments conducted in wet conditions, as well as for the hydration steps during cycling, a fraction of the

air flow was saturated passing through a temperature-controlled water bubble column (Variocool VC 1200 LAUDA). The dry air and humidified air were then mixed to obtain the targeted humidity value. The dry and humidified air flows were controlled by mass flowmeters (from Brooks, working in the 0–30 $NL.min^{-1}$ range). The humidity value was measured continuously downstream by means of a D2 General Eastern Chilled Mirror Hygrometer. The parameters were followed on-line on a monitor control implemented by means of a Siemens Sipart DR 20 S/K controller. The temperature was measured upstream and downstream of the reactor by means of Pt100 sensors and K-type thermocouples.

The pollutants were introduced in the multi-reactor device by mixing the main air flow with a nitrogen flow saturated with the pollutants' molecules, to reach the targeted pollutant concentration of 100 $mg.Nm^{-3}$ in a total flow of 1 $L.min^{-1}$. The nitrogen flow was saturated with each pollutant in a temperature-controlled bubbled column (at 25°C). The flow rate in each column was controlled by a GFC thermal mass flow controller (Aalborg). The concentration of the pollutant at the inlet and outlet of the reactors was measured by means of a flame ionisation detector (FID9000 Model, EPA) with a 1-min acquisition interval.

Twenty-four reactors were fed at the same time with the air/pollutant mixture. Each reactor was filled with 1 ± 0.02 g of sorbent (zeolite 13X or $MgSO_4$/13X composite). The use of 24 parallel and identical reactors made it possible to sample the material contained in one of the reactors while continuing the ageing (cycling) test on the others.

The following temperature program was applied during the cycling tests:

1. Hydration: isothermal step at 30°C for 90 min;
2. Dehydration: increasing temperature step (at 4°C/min rate) up to 165°C followed by an isothermal step at 165°C for 30 min;
3. Cooling/pre-adsorption step, decreasing the temperature step to 30°C in about 90 min.

These temperatures were chosen to represent as well as possible the real operating conditions

of the system in a building: 165°C it is a typical temperature that can be reached by evacuated tube solar air collectors, as explained in [23,24], and the 30°C temperature is close to the building inside air temperature during the discharging phase, and was chosen as it can be stabilised precisely from an experimental point of view. The 4°C/min rate was chosen for the temperature increase as it is of the same order of magnitude as the value that could be observed in a realistic system, as shown in [25].

Thirty-three cycles were performed on each sample with humid air and humid air/pollutant flows, to verify the impact of cycling and of the presence of pollutants on the storage materials. The number of cycles corresponded to the amount of pollutant that would pass through the reactor during different utilisation periods in a real application. Assuming an air flow estimated for a real installation for heating a single house (≈ 500 000 m^3/year) and the average air pollutant concentration reported in Table 1, one cycle in the multi-reactor device corresponds to 19 months use in a real installation, five cycles to 8 years, 10 cycles to 16 years and 33 cycles to 52 years use.

Table 1. Examples of organic and inorganic indoor/outdoor air pollutants and typical concentrations expressed in µg of pollutant per m^3 of air

Indoor pollutants			**Outdoor pollutants**		
Pollutant	Concentration ($\mu g.m^{-3}$)	Ref.	Pollutant	Concentration ($\mu g.m^{-3}$)	Ref.
Formaldehyde	19.4	[11]	Benzene	0.3	[28]
Hexaldehyde	17.0	[26]	Ethylbenzene	1.9	[29]
Nitrogen dioxide	32.5	[26]	Nitrogen dioxide	15.0	[28]
Styrene	2.1	[27]	Sulfur dioxide	1.0	[28]
Tetrachlorethylene	8.54	[27]	Toluene	12.9	[26]
Toluene	12.2	[26]	Xylene	0.9	[29]

2.3. Heat and water storage capacity measurements of the fresh and aged samples

The heat and water adsorption/desorption capacities of the fresh and cycled samples (in presence or absence of pollutants) were recorded using a Sensys TG-DSC (Thermogravimetry coupled to differential scanning calorimetry) apparatus, equipped with a Wetsys flow humidity generator, both from Setaram. Prior to the hydration process, the samples were dehydrated at the same temperature (165°C) as that applied during the cycles performed in the multi-reactor device described in section 2.2, by increasing the temperature from 30 to 165°C at 5°C min^{-1} under dry air flow (30 mL min^{-1}), followed by an isothermal step of 60 min at 165°C. The sample was then cooled at 30°C and hydrated under humid air ($\mathcal{H}$ = 60%). The hydration heat (kJ $g_{dry\ sample}^{-1}$) of the various samples was obtained by integration of the surface of the exothermic calorimetric peak obtained during hydration. The calorimetric and thermogravimetric signals were treated by mean of AKTS Advanced Thermokinetics software.

2.4. Physicochemical characterisations

Fourier-transform infrared spectroscopy (FTIR) was performed on the powders of the 13X and $MgSO_4$/13X samples by means of an FTIR iN10 MX (Thermo Scientific) analytical system.

Wavelength dispersive x-ray fluorescence (WDXRF) was performed in a Philips MagiX (2.4-kW) spectrometer to evaluate the Si/Al ratio in the fresh and cycled samples. Prior to analysis, the samples were shaped in pellets 13 mm in diameter and 1 mm thick by pressing the powders five 5 min, under 7-tonne pressure.

X-ray photoelectron spectroscopy (XPS) measurements were taken on a VG Scienta SES 2002 spectrometer equipped with a monochromatic Al Kα X-ray source (Al Kα = 1486.6 eV) and a hemispherical analyser. The XPS spectra were recorded with a pass energy of 100 eV and at 10^{-9} Pa pressure, in the analysis chamber; 24 mm^2 was the surface of the spot analysed and 9 nm the penetration depth of the x-ray photoelectrons. The binding energies (BEs) were calibrated on the basis of the C 1s peak (284.7 eV) of the atmospheric contaminant carbon. The peaks were fit using Gaussian-Lorentzian functions by means of the XPS-CASA software.

The surface area and porosity of the fresh and cycled samples were studied with a Micrometrics ASAP 2020 instrument by adsorbing N_2 at −196°C. CO_2 adsorption at 0 °C was also performed to finely investigate the microporosity. Prior to analysis, the samples were first pretreated at 130°C under vacuum for 12 h on the degas port and then again at 130°C for 2 h under vacuum on the analysis port. The free volumes were measured separately after analysis to avoid the pollution of the microporosity by He. The specific surface area (SSA) was calculated applying the BET (Brunauer, Emmett and Teller) theory [30] (within a range determined by the Rouquerol curve [31]), while the micropore volume (V_{micro}) was calculated by applying the t-plot method [32]. Finally, the pore size distribution was determined by applying the DFT model and considering the N_2 adsorption on an oxide surface and according to a cylindrical pore geometry. ^{27}Al magic angle spinning (MAS) nuclear magnetic resonance (NMR) spectroscopy spectra were recorded on a Bruker AVANCE II 400 MHz spectrometer. The 13X samples (fresh and cycled 33 times in presence of toluene) were analysed in a 2.5-mm-diameter cylindrical rotor at a 25-kHz spinning frequency.

3. Results and discussion

The aim of this study was to determine the impact of pollutant adsorption on the performance

of the storage system considered during the building's lifetime (at least 30 years of use), and to understand the cause of this impact by identifying the structural and morphological modifications that can occur on the solid storage material.

At first the adsorption capacity of 13X zeolite was determined for the three pollutants selected (toluene, styrene and hexanal) by acquiring the breakthrough curves, under dry and wet conditions (Table 2). These preliminary experiments were carried out only on the bare zeolite to verify the pollutants adsorption behaviour in presence of water vapour.

Table 2. Pollutant adsorption capacity on 13X zeolite in dry and wet conditions

Pollutant	**Concentration ($mg \cdot Nm^{-3}$)**	**Adsorption capacity ($mg \cdot g^{-1}$)**	
		H < 1%	H = 60%
Hexanal	100	575	1.0
Styrene	100	208	0.1
Toluene	100	113	1.1

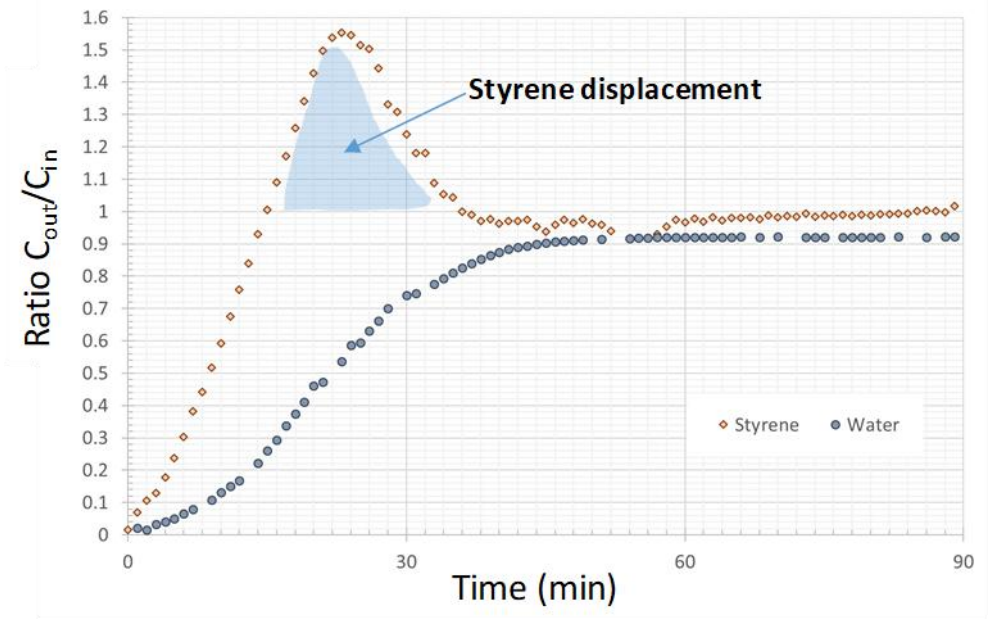

Fig. 3. *Styrene/water breakthrough curves in wet conditions at 30°C. C_{out} and C_{in},*

concentration at the exit and entrance of the reactor, respectively.

In dry conditions, the zeolites presented the highest adsorption capacity for hexanal, when compared to styrene and toluene; in wet conditions the total adsorption of all pollutants was drastically decreased by displacement phenomena: zeolite 13X shows a higher affinity for water that can then replace the pollutants' molecules, thus reducing their adsorption on the storage material [33, 34]. Figure 3 shows this behaviour for styrene (reported here as an example). At first, when all adsorption sites are free, the pollutant and the water molecules adsorb on the adsorbent (13X) at the same time. Then, when the number of free sites decreases, competition between styrene and water takes over, and water molecules displace the previously adsorbed styrene molecules, replacing them. This phenomenon is visualised by the light blue peak in Fig. 3, generated by a higher concentration of styrene on the out-stream flow (C_{out}) due to the release of the molecules of the pollutant displaced. The same behaviour was observed for the molecules of the three pollutants tested. This displacement behaviour has been previously reported in the literature [34, 35] and is called the "roll-over" phenomenon.

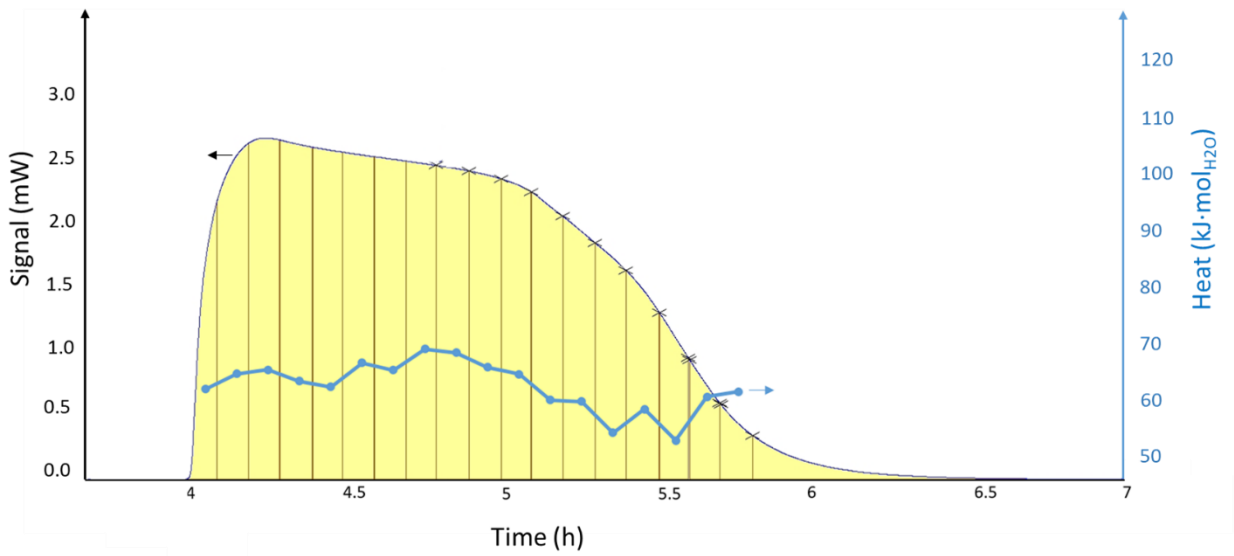

Fig. 4. *Hydration calorimetric curve for the 13X sample at 30°C and $\mathcal{H}$ =* 60%. *The surface in yellow represents the total hydration heat (in kJ·kg$^{-1}_{dry\ sample}$). The blue curve represents the average hydration energy (in kJ·mol$_{H2O}$) at the different time intervals.*

Even if the adsorption of the pollutants on the zeolite-based materials is strongly decreased due to the presence of water vapour during the hydration/dehydration cycles applied to the thermochemical storage system, the long-term impact (over several years' utilisation) needs to be investigated. Cycling tests were therefore performed under the experimental conditions detailed in Section 2.2 by means of the multi-reactor device shown in Fig. 2. Then the heat and water adsorption capacities of the fresh and cycled samples were measured in the TG-DSC apparatus as described in Section 2.3. The typical hydration curve is reported in Fig. 4 (for the 13X fresh sample, shown as an example). The integration of the surface under the curve (in yellow) represents the heat released (in kJ·kg$^{-1}_{dry\ sample}$). The results are compared in Fig. 5a, b, respectively, for the 13X and $MgSO_4$/13X samples cycled 1 and 33 times. In the case of the bare zeolite 13X, the heat of hydration of the sample cycled in presence of pollutants was always lower than that measured for the fresh 13X sample (see Fig. 5a).

Moreover, by increasing the number of cycles (from 1 to 33), the heat storage capacity (expressed as $kJ \cdot kg^{-1}_{dry\ sample}$) decreased further. A different behaviour was observed for the 13X sample cycled in presence of only water vapour (with no pollutant); in this case the zeolite presented higher hydration heat values. In contrast, even if the heat storage capacity of the $MgSO_4$/13X fresh sample, measured by calorimetry during hydration, was higher than that of the cycled samples, the material cycled 33 times showed a higher hydration heat than that cycled only once in presence of pollutants. The pollutant molecules seem to first strongly adsorb on $MgSO_4$/13X and then be displaced by the water molecules during the successive cycles, thus "reactivating" the sample that regains its initial heat storage capacity.

As a general trend, the negative effect of the pollutants on the heat storage capacity was in the styrene > hexanal > toluene order, on both samples. The decrease in heat storage capacity is directly correlated with the decrease in water sorption (Fig. 6a, b). The water molecules are adsorbed with similar energy on the sample whatever the coverage extent is, as illustrated in Fig. 4 for the 13X sample. The energy of water molecule adsorption on the 13X sample at different coverage extents (corresponding to different time intervals) is represented as the blue curve, and it is always around 60 $kJ \cdot mol^{-1}_{H2O}$.

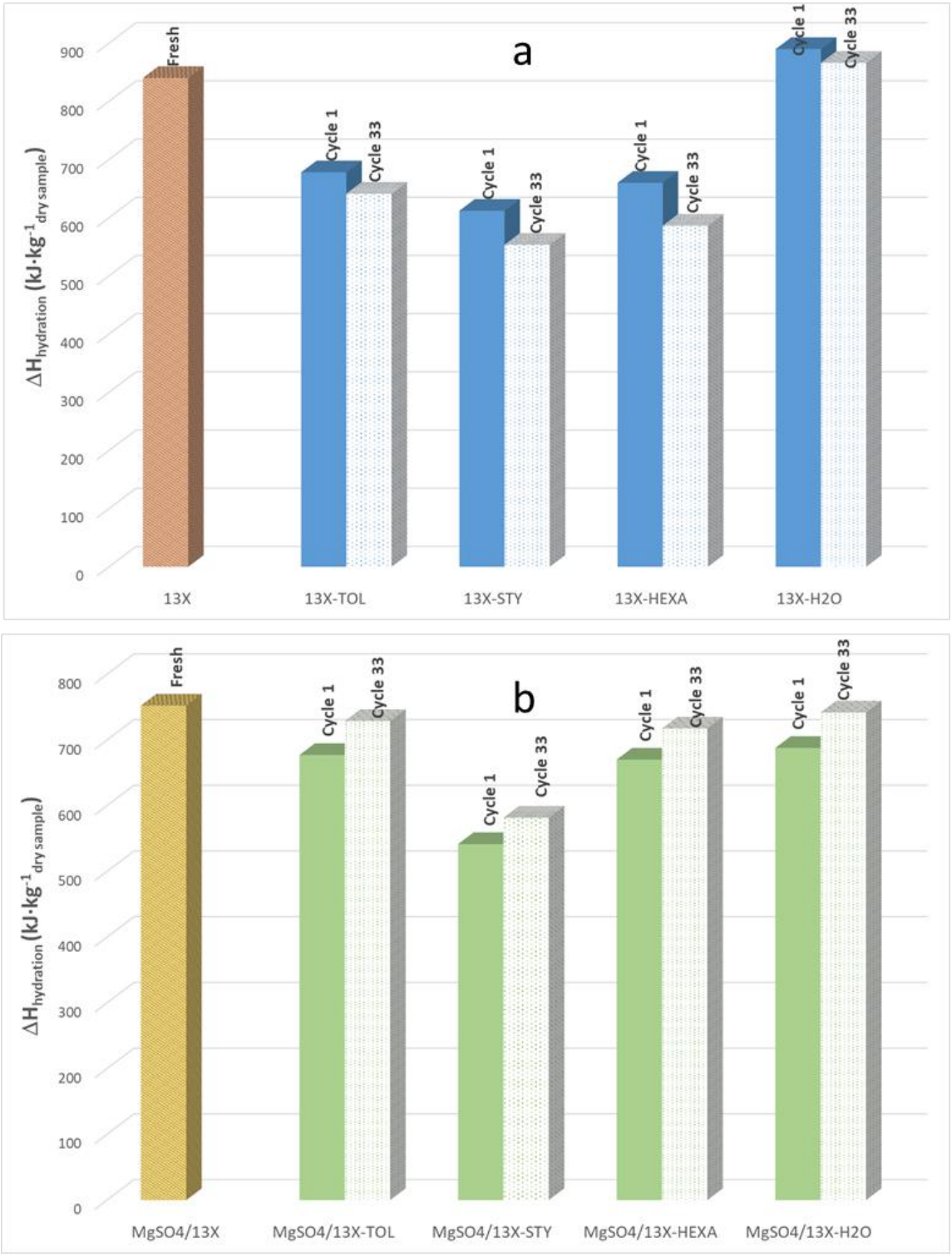

Fig. 5. *Hydration enthalpies for the 13X (a) and $MgSO_4$/13X (b) samples cycled 1 and 33 times (hydration performed at 30°C and $\mathcal{H}$ = 60%).*

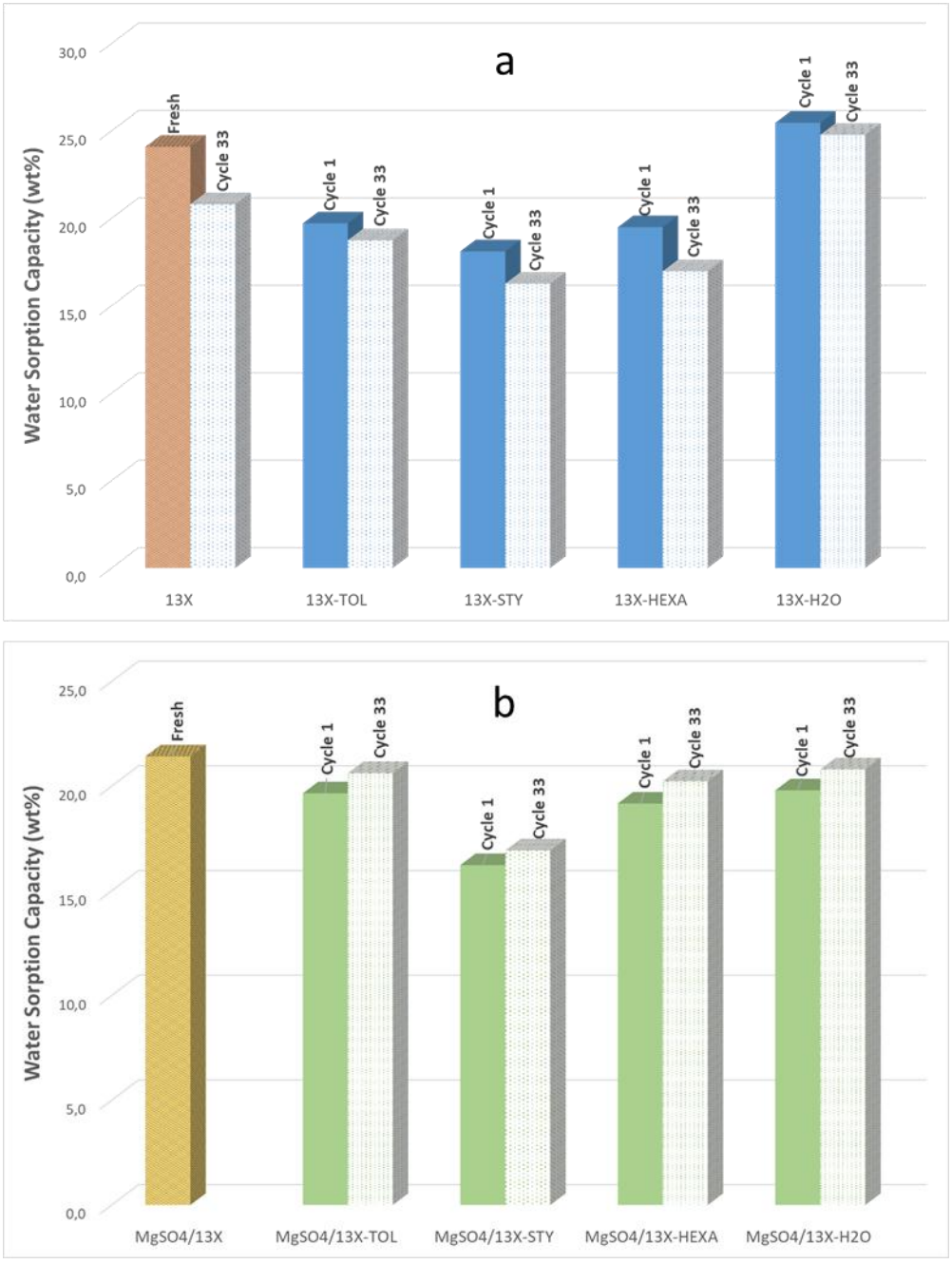

Fig. 6. *Water sorption capacity for the 13X (a) and $MgSO_4$/13X (b) samples cycled 1 and 33 times (hydration performed at 30°C and $\mathcal{H}$ = 60%).*

The samples were then characterised in detail to provide an understanding of the modification in the water sorption and heat capacity of the two samples after cycling in presence or absence of pollutants.

At first, the possible presence of pollutants accumulating on the samples' surface was checked

by IR spectroscopy and XPS analysis. No presence of the pollutants on the samples was detected. The FTIR spectra acquired for the 13X sample after cycling did not significantly differ from that of the fresh sample. In particular, neither stretching nor bending vibration peaks of the $–CH_2$ and –CO groups [36] of the adsorbed pollutants was observed, and the infrared spectra of the cycled 13X zeolites reported only the vibrations of the bare zeolite. The absence of the accumulation of pollutants on the samples' surface was also confirmed by XPS. Once again, the surface atomic composition of the fresh and cycled (in presence of styrene) 13X samples, did not differ. In particular, no accumulation of carbon-containing species was measured.

The decrease of the heat capacity and water up-take upon cycling is apparently not related to the deposition of pollutants on the heat storage material surface. The microstructure of the fresh and cycled 13X and $MgSO_4$/13X samples were then investigated by analysis of the N_2-adsorption isotherms acquired at −196°C. The main results are reported in Table 3 in terms of BET specific surface area (S_{BET}), micropore specific surface area (S_{micro}), total pore volume (V_{tot}) and micropore volume (V_{micro}), for all samples analysed. The N_2-adsorption isotherms are reported in Fig. 7 for the 13X samples cycled from 1 to 33 times in presence of pure water vapour (a), styrene (b) and for the $MgSO_4$/13X composite cycled in presence of styrene (c). Figure 8 represents the associated micropore distribution, and Fig. 9 the meso/macropore distribution.

The microstructure of zeolite 13X was clearly preserved during cycling with clean water vapour, as shown by the very low variation in the surface area and porous volume values. The associated isotherms (Fig. 7a) are all type I [37], typical of microporous samples with small external surface areas, for which the limiting nitrogen uptake is driven by the micropores' accessibility. The micropores' distribution (Fig. 8a) did not vary by cycling the sample in presence of pure water vapour, and no macroporosity was detected. The behaviour upon

cycling differed in presence of pollutants in the air flow: the specific surface area and porous volume of the samples decreased with the number of cycles (Table 3). This behaviour was not related to modification of the micropores distribution (determined by analysis of CO_2 adsorption isotherms) that did not vary for the samples cycled several times. In all cases, the type-I N_2-adsorption isotherm characterising the 13X zeolites changed towards type-IV isotherms (Fig. 7b for cycling in presence of styrene), with pronounced hysteresis, which can be associated with nitrogen capillary condensation into mesopores, typical of many industrial mesoporous adsorbents. These observations are also confirmed by the pore size distribution determined by analysis of the N_2-adsorption isotherm hysteresis (reported as an example in Fig. 8b and 9b for the cycles performed in presence of styrene), where a clear shift towards larger pores is observed. In particular, the appearance of meso/macroporosity is shown in Fig. 9b. The specific surface area of the $MgSO_4$/13X composite was much lower than that of the parent zeolite, due to the salt deposition that, blocking the micropores' access, diminished the access and adsorption of nitrogen molecules, as already reported in the literature [11]. After the first cycle, the salt distribution and arrangement probably was modified due to the hydration/dehydration phenomena letting supposing that the new salt space configuration free the pore access; then nitrogen could reach the pores and the porous volume, and the S_{BET} measurement significantly increased. The $MgSO_4$/13X sample was less affected by the presence of pollutants (Table 3) and all N_2-adsorption isotherms of the cycled samples were type I; no creation of macro/mesoporosity was observed (Fig. 9). Only the presence of styrene impacted the impregnated zeolite at a higher level, for which the specific surface and micropore volume decreased from 489 to 258 $m^2 \cdot g^{-1}$, respectively, and from 0.17 to 0.09 $cm^3 \cdot g^{-1}$ between cycle 1 and cycle 33 (Table 3).

Table 3. Microstructural properties of the fresh and cycled 13X and $MgSO_4$/13X samples determined from N_2-adsorption isotherms

Sample / ***Pollutant***	***13X***					***$MgSO_4$/13X***				
	Cycle n.	***S_{BET}[a] ($m^2 \cdot g^{-1}$)***	***S_{micro}[b] ($m^2 \cdot g^{-1}$)***	***V_{tot} ($cm^3 \cdot g^{-1}$)***	***V_{micro} ($cm^3 \cdot g^{-1}$)***	***Cycle n.***	***S_{BET}[a] ($m^2 \cdot g^{-1}$)***	***S_{micro} ($m^2 \cdot g^{-1}$)***	***V_{tot} ($cm^3 \cdot g^{-1}$)***	***V_{micro}[b] ($cm^3 \cdot g^{-1}$)***
-	**-**	**662**	**612**	**0.28**	**0.23**	-	**367**	**330**	**0.22**	**0.17**
Pure water vapour	1	647	602	0.28	0.23					
	4	670	629	0.28	0.24					
	33	668	620	0.28	0.23					
Toluene	1	424	415	0.18	0.18	1	517	481	0.23	0.18
	5	318	272	0.22	0.22	5	466	433	0.21	0.16
	10	244	201	0.23	0.23					
	33	179	139	0.17	0.17	33	499	462	0.23	0.17
Styrene	1	341	339	0.13	0.13	1	489	457	0.22	0.17
	5	331	298	0.24	0.24	5	430	399	0.21	0.15
	10	360	313	0.24	0.24					
	33	238	196	0.18	0.18	33	258	228	0.14	0.09
Hexanal						1	492	457	0.22	0.17
						4	477	443	0.22	0.17
	5	401	346	0.23	0.23					
	10	211	182	0.16	0.16					
	33	179	139	0.17	0.17	33	439	405	0.19	0.15

[a] *Calculated by applying the BET equation [32]*

[b] *Calculated using t-plot method [32]*

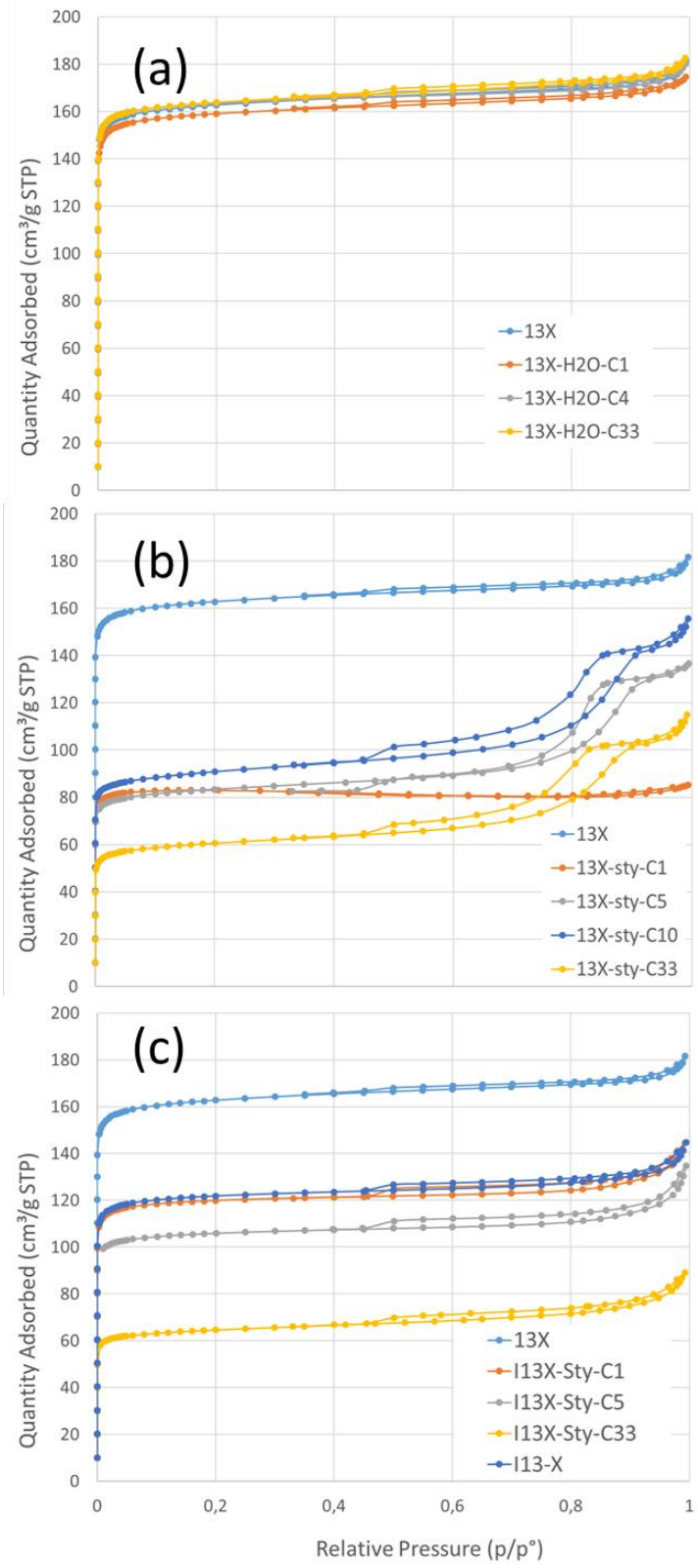

Fig. 7. *N_2-adsorption isotherm for the 13X samples cycled from 1 to 33 times in presence of pure water vapour (a), styrene (b), and for the $MgSO_4$/13X composite cycled in presence of styrene (c), respectively.*

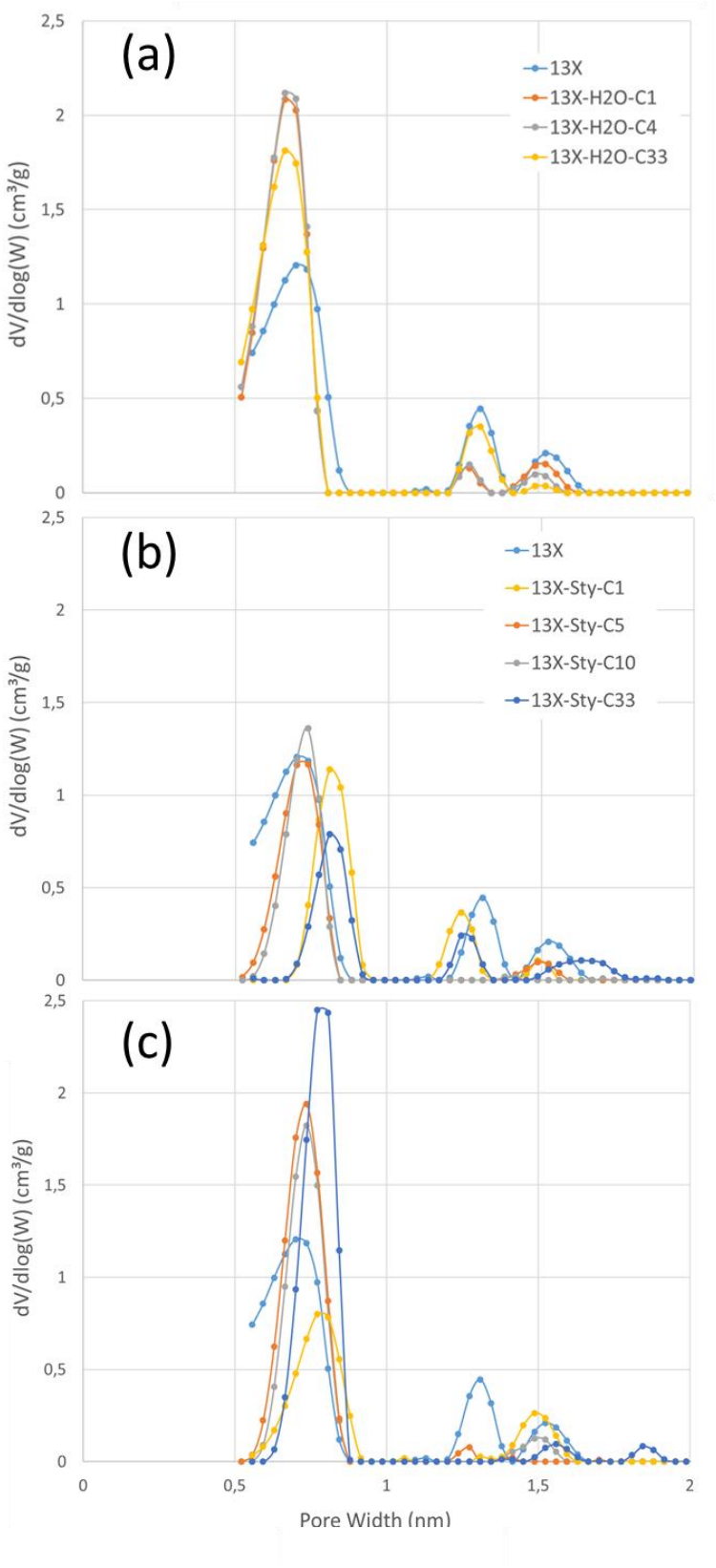

Fig. 8. *Micropore for the 13X samples cycled from 1 to 33 times in presence of pure water vapour (a), styrene (b), and for the $MgSO_4$/13X composite cycled in presence of styrene (c), respectively.*

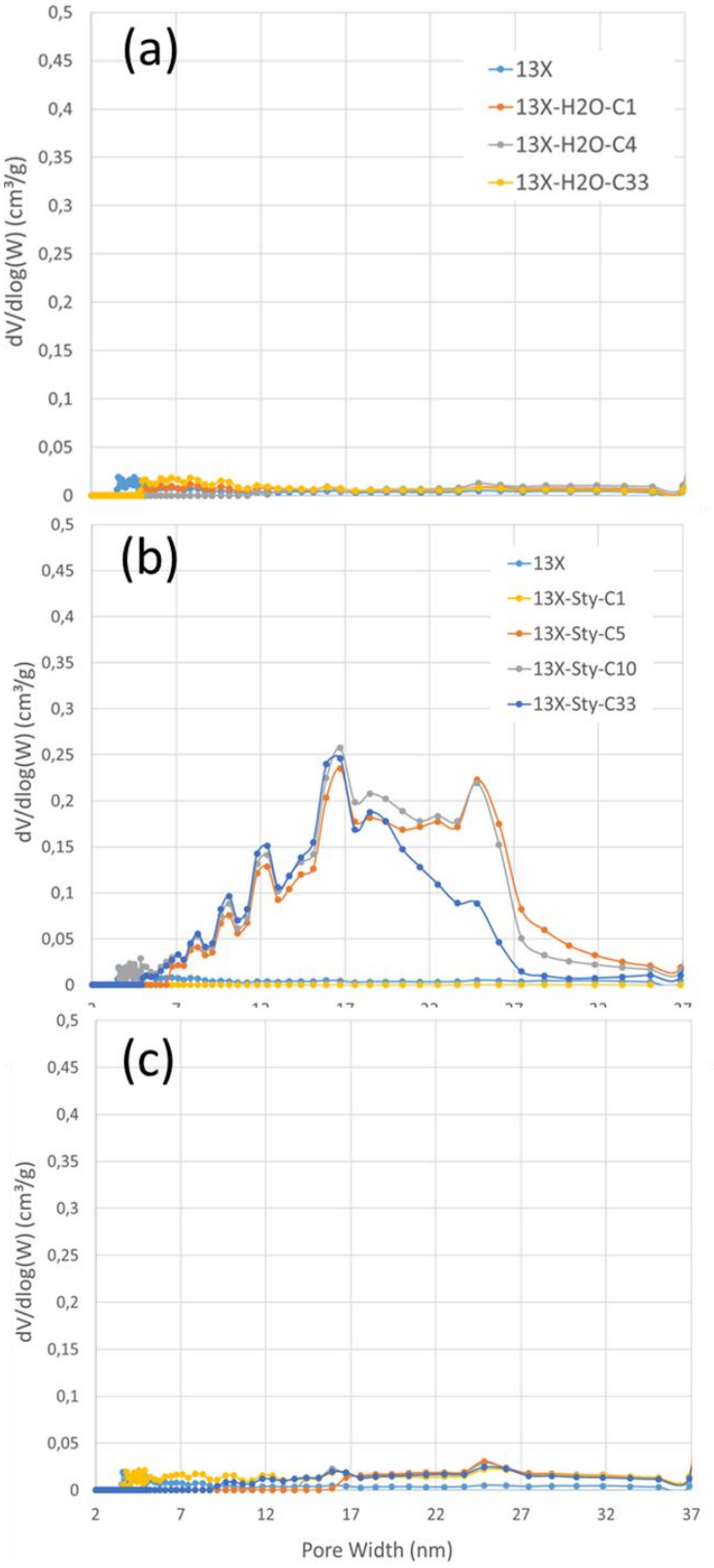

Fig. 9. *Meso/macropore for the 13X samples cycled from 1 to 33 times in presence of pure water vapour (a), styrene (b), and for the $MgSO_4$/13X composite cycled in presence of styrene (c), respectively.*

The modification in the samples' microstructure (in particular for the 13X sample upon cycling) could not be assigned to pollutant accumulation on the sample surface, as shown by XPS and FTIR analysis. Then the bulk sample composition was analysed using WDXRF for the 13X fresh and cycled samples. This investigation was inconclusive and a constant value of 1.25 for the Si/Al ratio was measured for all samples. Indeed, even if in-situ de-alumination takes over during cycling, no mass transfer is involved in the process and the extracted aluminium might remain in the sample matrix, thus resulting in an unmodified Si/Al ratio.

To finally verify the true chemical environment of aluminium atoms in the 13X zeolite, ^{27}Al NMR spectra were acquired for the fresh sample and the sample cycled 33 times in presence of toluene (Fig. 10a, b, respectively). A main peak at an approximately 60-ppm chemical shift was visible on both samples and assigned to tetrahedrally coordinated aluminium atoms ($Al(OSi)_4$) [38], connected to the main zeolite structure. In case of de-alumination, octahedrally coordinated aluminium is present in extra-framework positions in the zeolite matrix. In the 13X zeolite cycled 33 times in presence of toluene (13X-Tol sample), a weak peak at around 3 ppm confirms the presence of de-alumination, even if to a small extent.

Slow de-alumination undertaken by cycling in presence of water vapour and pollutants therefore seems to be the cause of the modification of the microstructure of the 13X sample and to the related loss in heat storage capacity and water uptake. The presence of $MgSO_4$ appears to protect the zeolite from de-alumination, and hydration/dehydration cycling on the $MgSO_4$/13X sample, even in presence of pollutants, does not have a strong effect on the sample's microstructure, probably because the pollutants cannot reach the internal pores, due to blockage of the pores' access by the salt deposited.

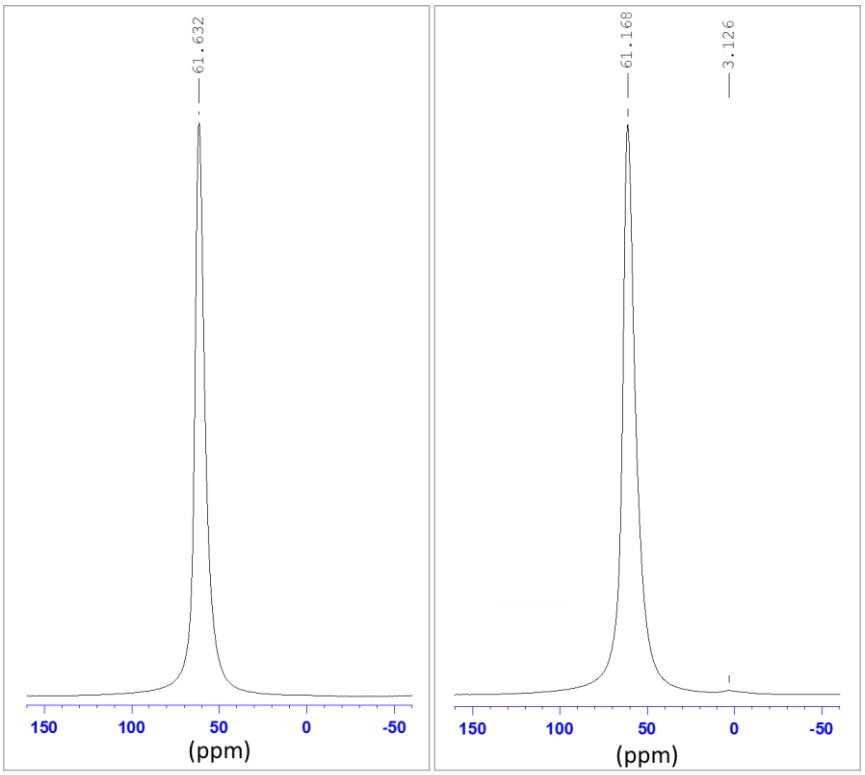

Fig. 10. *^{27}Al MAS NMR spectra of (a) 13X and (b) 13X cycled 33 times in presence of toluene samples.*

4. Conclusions

Zeolite-based heat storage materials are confirmed to be a very good option for open sorption thermochemical heat storage systems, even when the carrier gas (air) is polluted by organic molecules such as toluene, styrene and hexanal. The strong affinity of zeolite 13X and $MgSO_4$/13X composite for water allows displacement processes of the pollutant molecules that help to avoid the fast poisoning of the solid material, thus enhancing their durability (in terms of maintaining the heat capacity). Nevertheless, during several years' utilisation, hydration/dehydration cycling in presence of pollutants can modify the microstructure in the zeolite framework, due to slow and long-term de-alumination phenomena, and the consequent decrease in the heat storage capacity and water sorption. The impact of pollutants has been demonstrated to be stronger on the pure zeolite, while the deposited salt ($MgSO_4$) seems to protect the material surface from the pollutant effect, and no dramatic microstructural modifications could be detected on the salt-containing composite.

The choice of pure zeolites or composites (prepared by impregnating the zeolites with various salts, such as $MgSO_4$ as in the present research) for implementation in a thermochemical heat storage device must then be made not only by comparing the intrinsic heat storage capacity of the materials measured in ideal conditions (absence of pollutants), but taking into account the average concentration of organic molecules in the air stream that will be used in the actual installation. In ideal conditions, bare zeolite remains the best choice in terms of total heat storage, but addition of an optimised amount of hydrated salts can improve the durability of the storage material and the long-term efficiency of the thermochemical heat storage systems.

Funding: - Région Auvergne Rhône Alpes for the PhD thesis grant of T. Polimann

- Région Grand Est for providing funding for the acquisition of the TG-DSC equipment within the "STOCKFATAL project.

- Carnot MICA and Energies du futur Institutes, for funding the Projet InterCArnot "StockEner".

Acknowledgements

The authors would like to thank the Carnot Institutes MICA and Energies du futur (France) for supporting a part of this study within the STOCKENER project; Region Grand Est (France) for providing funding for the acquisition of the TG-DSC equipment in the STOCKFATAL project; and Region Auvergne Rhône-Alpes for the PhD thesis grant of T. Polimann.

All physicochemical characterisations were performed on the IS2M technical platforms. The authors are very grateful to S. Hajjar (XPS) and L. Michelin (XRF) for their contribution.

Liste of References

[1] Aydin D, Casey SP, Riffat S. The latest advancements on thermochemical heat storage systems. Renew Sustain Energy Rev 2015;41:356–67. doi: 10.1016/j.rser.2014.08.054

[2] Yan T, Wang RZ, Li TX, Wang LW, Fred IT. A review of promising candidate reactions for chemical heats storage. Renew Sustain Energy Rev 2015;43:13–31. doi: 10.1016/j.rser.2014.11.015

[3] Kuznik F, Johannes K, Obrecht C, David D. A review on recent developments in physisorption thermal energy storage for building applications. Renew Sustain Energy Rev 2018;94:576-86. doi: 10.1016/j.rser.2018.06.038

[4] Shah SK, Lu A, Rismanchi B. Seasonal thermal energy storage system for cold climate zones: A review of recent developments. Renew Sustain Energy Rev 2018;97:38-49. doi: 10.1016/j.rser.2018.08.025

[5] N'Tsoukpoe KE, Liu H, Le Pierrès N, Luo L. A review on long-term sorption solar energy storage. Renew Sustain Energy Rev 2009;13:2385-96. doi: 10.1016/j.rser.2009.05.008

[6] Hadorn JC, 2011. Solar and Heat Pump Systems - Status of the IEA SHC Task 44 & HPP Annex 38. In: Proc. of the ISES Solar World Congress 2011, Aug. 28 - Sep. 2, Kassel, Germany.

[7] van Essen VM, Zondag HA, CotGores J, Bleijendaal L.P.J., Bakker M, Schuitema R, van Helden WGJ, He Z, Rindt CCM. Characterization of $MgSO_4$ hydrate for thermochemical seasonal heat storage. J Solar Energ Eng (ASME) 2009;131:041014-1–041014-7. doi: 10.1115/1.4000275

[8] Tatsidjodoung P, Liu H, Le Pierrès N, Luo L. A review on long-term sorption solar energy storage. Renew Sustain Energy Rev 2013;18:327-49. doi: 10.1016/j.rser.2009.05.008

[9] Jänchen J, Stach H, Shaping adsorption properties of nano-porous molecular sieves for

solar thermal energy storage and heat pump applications, Sol. Energy 2014;104:16–18. doi: 10.1016/j.solener.2013.07.018

[10] Chen L, Ondarts M, Outin J, Gonthier Y, Gonze E. Catalytic decomposition performance for O_3 and NO_2 in humid indoor air on a MnO_x/Al_2O_3 catalyst modified by a cost-effective chemical grafting method. J. Environm. Sc. 2008;74:58-70. doi: 10.1016/j.jes.2018.02.006

[11] Kirchner S, Arènes JF, Cochet C, Derbez M., Duboudin C, Elias P, Grégoire A, Jédor B, Lucas JP, Pasquier N, Pigneret M, Ramalho O. Etat de la qualité de l'air dans les logements français. Environnement, Risques & Santé, 6/4, juillet-août 2007; 250-69 [doi : 10.1684/ers.2007.0096]

[12] Sundell J. On the history of indoor air quality and health. Indoor Air 2004;14:51-58. doi: 10.1111/j.1600-0668.2004.00273.x

[13] Edwards RD, Jurvelin J, Koistinen K, Saarela K, Jantunen M. VOC source identification from personal and residential indoor, outdoor and workplace microenvironment samples in EXPOLIS-Helsinki, Finland. Atmospheric Environm. 2001;35:4829-4841. doi: 10.1016/S1352-2310(01)00271-0

[14] Brosillon S, Manero M-H, Foussard J-N. Mass Transfer in VOC Adsorption on Zeolite: Experimental and Theoretical Breakthrough Curves. Environ. Sci. Technol. 2001;35:3571–3575. doi: 10.1021/es010017x

[15] Lee D-G, Kim J-H, Lee C-H. Adsorption and thermal regeneration of acetone and toluene vapors in dealuminated Y-zeolite bed. Separation and Purification Technol. 2011;77:312–324. doi: 10.1016/j.seppur.2010.12.022

[16] Helaly HO, Awad MM, El-Sharkawy II, Hamed AM. Theoretical and experimental investigation of the performance of adsorption heat storage system. Appl. Therm. Eng. 2019;147:10-28. doi: 10.1016/j.applthermaleng.2018.10.059

[17] Henninger SK, Ernst S-J, Gordeeva L, Bendix P, Frohlich D, Grekova AD, Bonaccorsi L, Aristov Y, Jaenchen J. New materials for adsorption heat transformation and storage. Renew. Energy 2017;110:59-68. doi: 10.1016/j.renene.2016.08.041

[18] Visscher K, Veldhuis JBJ, Oonk HAJ,vanEkeren PJ, Blok JG. Compacte Chemische Seizoenopslag Van Zonnewarmte; Eindrapportage, ECN Report no. ECN-C-04-074, 2004.

[19] Whiting G, Grondin D, Bennici S, Auroux A. Heats of water sorption studies on zeolite–MgSO4 composites as potential thermochemical heat storage materials. Solar Energy Materials & Solar Cells 2013;112:112–119. doi: 10.1016/j.solmat.2013.01.020

[20] Hongois S, Kuznik F, Stevens P, Roux J-J. Development and characterisation of a new $MgSO_4$-zeolite composite for longterm thermal energy storage. Solar Energy Materials and Solar Cells 2011;95:1831–1837. doi: 10.1016/j.solmat.2011.01.050

[21] Lee D-G, Kim J-H., Lee C-H. Adsorption and thermal regeneration of acetone and toluene vapors in dealuminated Y-zeolite bed. Separation and Purification Technology 2011;77:312–324. doi: 10.1016/j.seppur.2010.12.022

[22] Barson CA, Knight JR, Robb JC, 1972. The polymerisation of styrene on 13X zeolite. British Polymer Journal 1972;4:427–435. doi: 10.1002/pi.4980040506

[23] Kuznik F, Gondre D, Johannes K, Obrecht C, David D. Numerical modelling and investigations on a full-scale zeolite 13X open heat storage for buildings. Renewable Energy 2019;132:761-772. doi: 10.1016/j.renene.2018.07.118

[24] Tatsidjodoung P, Le Pierrès N, Heintz J, Lagre D, Durier F. Experimental and numerical investigations of a zeolite 13X/water reactor for solar heat storage in buildings. Energy Conversion and Management 2016;108:488-500. doi: 10.1016/j.enconman.2015.11.011

[25] Tatsidjodoung P, Procédé de stockage d'énergie solaire thermique par adsorption pour le chauffage des bâtiments : Modélisation et Simulation numérique. PhD thesis of Grenoble University. 26 May 2014.

[26] Mosqueron L, Nedellec V. Hiérarchisation sanitaire des paramètres mesurés dans les bâtiments par l'observatoire de la qualité de l'air intérieur. Technical report, Observatoire de la Qualité de l'Air Intérieur, 2002.

[27] Bonanno LJ, Freeman NCG, Greenberg M, Lioy PJ. Multivariate Analysis on Levels of Selected Metals, Particulate Matter, VOC, and Household Characteristics and Activities from the Midwestern States NHEXAS, Appl. Occupational Environ. Hygiene. 2001;16;859-874. doi: 10.1080/10473220121418

[28] Bentayeb M, Stempfelet M, Wagner V, Zins M, Bonenfant S, Songeur C, Sanchez O, Rosso A, Brulfert G, Rios I, Chaxel E, Virga J, Armengaud A, Rossello P, Rivière E, Bernard M, Vasbien F, Deprost R. Retrospective modeling outdoor air pollution at a fine spatial scale in France. Atmospheric Environm. 2014;92;267-279. doi: 10.1016/j.atmosenv.2014.04.019

[29] Roukos J, Riffault V, Locoge N, Plaisance H. VOC in an urban and industrial harbor on the French North Sea coast during two contrasted meteorological situations. Environm. Pollut. 2009;157:3001–3009. doi: 10.1016/j.envpol.2009.05.059

[30] Brunauer S, Deming L, Deming WE, Teller E. On a theory of the van der Waals adsorption of gases. J American Chem Soc 1940;62:1723-32. doi: 10.1021/ja01864a025

[31] Thommes M, Kaneko K, Neimark AV., Olivier JP, Rodriguez-Reinoso F, Rouquerol J, Sing KSW. Physisorption of gases, with special reference to the evaluation of surface area and pore size distribution (IUPAC Technical Report). Pure Appl. Chem. 2015; 87: 1051–1069. doi: 10.1515/pac-2014-1117

[32] Lowell S, Shields JE. Ch.9 Microporosity in "powder surface area and porosity book".

1984. Printed in Great Britain by J.W. Arrowsmith Ltd, Bristol. ISBN 0412252406. doi: 10.1007/978-94-009-5562-2

[33] Tao W-H, Yang TC-K, Chang Y-N, Chang L-K, Chung T-W. Effect of moisture on the adsorption of volatile organic compounds by zeolite 13X. J Environ Eng. 2004;130:1210-16. doi: 10.1061/(ASCE)0733-9372(2004)130:10(1210)

[34] Azambre B, Westermann A, Finqueneisel G, Can F, Comparot JD. Adsorption and Desorption of a Model Hydrocarbon Mixture Over HY Zeolite Under Dry and Wet Conditions. J. Phys. Chem. C 2015;119:315−331. doi: 10.1021/jp509046n

[35] Gong R, Keener TC. A qualitative analysis of the effects of water vapor on multi-component vapor-phase carbon adsorption. Air & Waste 1993;43:864-872. doi: 10.1080/1073161X.1993.10467169

[36] Ozturk N, Ucun F, Muhtar A D, Bahceli S. Infrared and SEM analyses of polyethyleneglycol-400 adsorbed on zeolites NaA, CaA, NaX and NaY. J. Molec. Struc. 2009;922:35-38. doi: 10.1016/j.molstruc.2009.01.038

[37] Sing KSW. Reporting physisorption data for gas/solid systems with special reference to the determination of surface area and porosity. Pure & Appl Chem 1982;54:2201-18. doi: 10.1351/pac198254112201

[38] Muller M, Harvey G, Prins R. Quantitative multinuclear MAS NMR studies of zeolites. Microp. Mesop. Mat. 2000;34:281-90. doi: 10.1016/S1387-1811(99)00180-8